



## Development of High Performance Multi-Axial Hybrid Simulation System for Full-scale Testing

X. Shawn Gao<sup>1</sup>, Shawn You<sup>1</sup>, Arturo Schultz<sup>2</sup>, Paul Bergson<sup>2</sup>

<sup>1</sup> MTS Systems Corporation – Eden Prairie, MN, USA.

<sup>2</sup> Department of Civil, Environmental, and Geo-Engineering, University of Minnesota - Minneapolis, MN, USA.

### ABSTRACT

The hybrid simulation technique has been widely used for structural testing in the past two decades. To evaluate realistic structural performance under extreme environmental loadings, the University of Minnesota Multi-axial Sub-assembly Testing (MAST) facility has recently been upgraded to perform multi-axial hybrid simulation. MAST is among very few systems in the world which is capable of three-dimensional six-degree-of-freedom loading on full-scale structural components, from the initial linear elastic state until collapse. Moreover, the unique actuator hydrostatic bearing design enables ultra-low friction, making the system ideal to perform high performance hybrid simulation without the necessity of laborious friction compensation efforts. Friction could be a major challenge for multi-axial loading system of such size, which could cause hybrid system instability if not properly managed. A suite of validation tests are performed using the MAST system, with all 6 degree-of-freedom participating in the hybrid simulation working mode. The physical substructure is a 5.5-meter tall full-scale W12×190 ASTM 572 Gr. 50 steel column, and all other elements of a 3-story moment resisting frame structure are modelled in OpenSees. First, the earthquake records are scaled to keep the specimen response within the linear elastic region, and in which the hybrid simulation exhibits excellent correlation with analytical predictions. The system shows strong repeatability and robustness under various maximum amplitude and loading rate combinations. The friction measured in the system is negligible compared with restoring forces for the specimen. Finally, the specimen is tested to nonlinear and yield under the full-scale Northridge earthquake records, which demonstrates that the MAST system has full potential for high performance assessment of complex nonlinear structures.

Keywords: Hybrid Simulation, MAST, Full-scale Testing, Friction

### INTRODUCTION

Physical testing of structures and components for earthquake loads are typically conducted using either quasi-static testing or hybrid simulation. An advantage to quasi-static testing is the use of “real” structural elements that, due to the slow loading technique, allows observation of failure and specimen behavior. However, a major limitation of this technique is the inability to simulate a particular earthquake. The Multi-Axial Sub-Assembly Testing (MAST) Laboratory at the University of Minnesota, Twin Cities (**Figure 1**) with partial funding from the National Science Foundation (NSF) as part of the George E. Brown Network for Earthquake Engineering Simulation (NEES), was developed to overcome these limitations. The MAST system is a large-scale test apparatus for quasi-static and hybrid simulation of structures and components [1].

### MAST Testing Apparatus

The MAST apparatus (**Figure 1**) is a self-restraining system with 4 vertical actuators spanning from the crosshead to the strong floor, and with the 2 actuators reacting against the L-shaped reaction wall in each orthogonal horizontal direction. The steel crosshead spans 8930 mm from tip to tip, weighs 418 kN and is formed by 1420-mm wide by 1650-mm deep stiffened steel box sections. The strong floor comprises a 2,290-mm thick concrete slab with a 140-mm thick top steel plate, the latter which has threaded holes at a 460-mm (230-mm below the crosshead) spacing to enable attachment of test specimens. The post-tensioned concrete slab has 10.67m orthogonal horizontal dimensions and is supported by a group of 64 piles that are driven to bedrock. The reaction wall is 10.67-m tall, and each 2,130-mm thick wing is post-tensioned to the strong floor and to each other. The wall has through-holes spaced at 460 mm to enable attachment of the horizontal actuators, ancillary actuators or other fixtures. The resulting payload dimensions are 6.10 m along the longitudinal and transverse horizontal directions, and 9.14 m vertically.

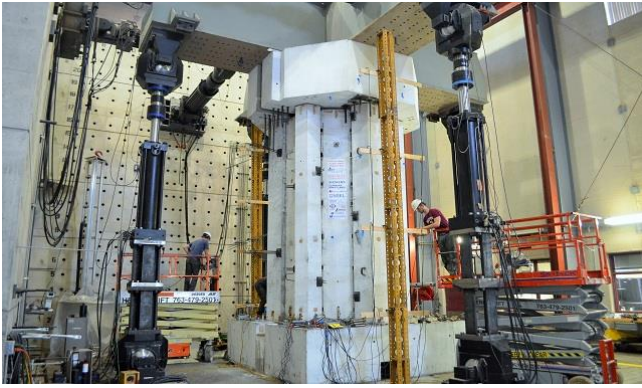


Figure 1: MAST system with a structural specimen

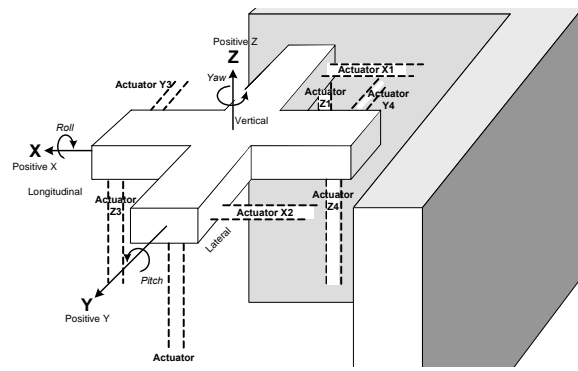


Figure 2: Schematic of the MAST global DOFs

The MAST can deliver large forces and strokes at the top of the specimens (i.e. bottom of the crosshead) in 6 spatial degrees of freedom (DOF) at the crosshead. The DOFs are defined in global coordinates as shown in **Figure 2**, and force and stroke capacities for the global translation DOFs are summarized in **Table 1**. Given the large forces that the vertical actuators can carry, hydraulic bearings are used at both ends of all vertical actuators to reduce friction to a negligible amount. Additionally, the ancillary actuators (not shown in **Figure 1**) can be used to provide additional loading beyond that required for control of the global DOFs. Besides the forces given in Table 1, each wing of the strong wall has been designed to resist simultaneous application of 3,900-kN forces at 4.88 and 9.76 m heights above the base, as well as develop simultaneous, out-of-plane moments equal to 59,100kN-m, and a maximum vertical twist of 51,500 kN-m. Each threaded hole in the floor and through-hole in the wall can develop 555-kNs of simultaneous shear and axial force. Maximum relative deflection of the crosshead under full load is 2.5 mm, and maximum lateral deflection of the wall is 12.5 mm (out-of-plane).

Table 1: MAST system capacities

Global DOF	Force	Stroke	Swivel Rotation
vertical	6.0 MN	±500 mm	±30°
longitudinal	4.0 MN	±400 mm	±25°
transverse	4.0 MN	±400 mm	±25°
ancillary	4.0 MN	±250 mm	---

The MAST is controlled by a shake-table controller that has been customized for movement of the crosshead. The user can specify target input values as either a global position or a global load. Through coordination of these components, the system establishes control of the crosshead as a plane in space, which makes it possible to apply tri-axial control to three-dimensional structures, as well as application of planar translations to planar substructures. It is also possible to control the crosshead in mixed mode, setting some of the degrees of freedom in load control and others in displacement control. DOFs can also be configured in linear slaving relationships (i.e. link one DOF to another DOF) to the feedback signal of independent DOF's. Other sophisticated features include: 1) the ability to change the mode of control in a DOF from one loading step to the next, 2) the internal calculation for the influence of the changing geometries of the actuators as the test specimens deform, and 3) the internal compensation for the use of four vertical actuators when three are sufficient to define a plane in space. The MAST system also now offers hybrid simulation capabilities, using ramp-and-hold load incrementing, in conjunction with the OpenFresco freeware and several common finite element platforms such as OpenSEES [2]. Robust data acquisition is available which, in addition to collecting sensor data, also collects the DOF and ancillary actuator feedbacks from the analog outputs of the MTS controller.

### Past Projects

The MAST Lab operated as part of the NSF NEES program for fifteen years, during which time a wide variety of projects were conducted. Since the end of the NSF NEES program, the MAST Lab has continued operating as part of the U of MN CSE and Dept of CECE for structural testing needs of the faculty as well as faculty at other institutions. Three past projects are briefly mentioned here with focus on the control scheme even though these predated the hybrid simulation update of the MAST Lab in 2018. In particular, the use of computed channels is highlighted. For example, moment on the test structure can be controlled as a function of the applied shear (i.e. horizontal force in the principal direction) of the test specimen, or a P-Delta input moment can be defined as the linear combination of a lateral displacement in one DOF and the weight.

A recent project focused on tall towers for wind energy production [3]. Wind turbine towers with hub heights of 100-m and higher (up to 140-m) enable access to more constant wind flows that have higher speeds, thus reducing energy production costs. The Hexcrete tower concept (**Figure 1**) is a post-tensioned system using high-strength concrete (HSC) and/or ultra-high performance concrete (UHPC). The research conducted at the MAST Lab served as a proof test of a full-scale Hexcrete tower cell to validate the design process. The test specimen was subject to operational, extreme and ultimate loading protocols defined as combinations of top drifts in the longitudinal and transverse horizontal directions (DOFs  $X$  and  $Y$  in **Figure 2**), moments about these axes that were proportional to orthogonal horizontal shear forces needed to produce the target drifts, torsional moment about the vertical axis (DOF  $Z$  in **Figure 2**), and a constant vertical load representing the weight of the tower above the cell. Overturning moments about the  $X$ - and  $Y$ -axes approaching 10,000 kN-m were generated, as well as torsional moment approaching 8,000 kN-m to produce 4 degree of rotational twist. The testing validated the tower design to resist both operational and extreme loads, and that the test unit had sufficient ductility and load capacity beyond extreme loading levels.

An earlier project (**Figure 3**) investigated the seismic performance of special truss moment frames (STMFs) given their ability to achieve large column-free floor spaces [4]. The STMF system was originally developed for low seismic regions, but the high lateral stiffness and light weight make this system attractive for use in high seismic regions. STMFs can dissipate earthquake energy through special ductile segments located near the mid-span of the truss girders, while the other members outside the special segment can be designed to remain elastic. Full-scale tests of two STMF subassemblages were conducted at the MAST Lab, with the global coordinate system rotated 45 degrees about the vertical axis ( $Z$  axis in **Figure 2**) to enable 7.26-m long specimens to be tested. The specimens were loaded using a cyclic drift applied by the MAST crosshead, through a load transfer beam, in the longitudinal direction of the frame (**Figure 3**). Displacement in the transverse direction was constrained to zero to maintain out-of-plane stability, and rotations about the longitudinal and vertical axes of the specimens were also constrained to zero. The overturning moment, i.e. about the transverse frame axis, was slaved to the force applied in the longitudinal direction. The tests of the STMFs at the MAST Lab were conducted over a range of top lateral drifts that exceeded  $\pm 0.2$  m until the STMF specimens lost most of their lateral load capacity.



**Figure 3:** Special truss moment frame (STMF) test



**Figure 4:** Two-story steel braced frame test

Another project at the MAST Lab utilized three-dimensional, near full-scale test specimens (**Figure 4**) of a special concentrically braced frame (SCBF) and buckling-restrained braced frame (BRBF) [5]. The two specimens were configured with braces in two orthogonal bays framing into a “shared” column with a floor system designed and constructed to simulate realistic conditions. The first specimen, the SCBF, employed braces in an X-configuration, and the second test specimen, the BRBF, employed pin-ended, collared BRBs in a single-diagonal configuration. Cyclic lateral displacements at the top of the specimens were applied bi-directionally in an unsymmetric “cloverleaf” configuration in the  $X$  and  $Y$  directions (**Figure 2**), and the torsional rotation ( $Z$  axis in **Figure 2**) of the crosshead was maintained at zero to prevent torsional deformation at the top of the frame. No overturning moments about the  $X$  and  $Y$ -axes (**Figure 2**) were applied by the crosshead. Another interesting feature of this study is that the MAST apparatus was used not only for the testing, but to support the frame structure as it was being fabricated inside the MAST Lab. This study determined that the drift capacity of the SCBF test frame was only 6% less than that of comparable planar frames while the ductility capacity of the BRBF exceeded that of many of the planar BRBF system tests.

## Hybrid Simulation Testing Upgrade

In complicated multi-axial testing, each actuator position is in its local coordinate system, while the test specimen position is specified in global Cartesian coordinate system. MTS DOF control software [6] provides coordinate transformation in which actuators act in groups to produce the global specimen movement in up to six degrees of freedom. The actuator feedbacks (load, displacement, acceleration, and optionally the differential pressure) are converted from actuator signals through DOF software into global coordinates, and the controller closes the loop using these DOF coordinates. The DOF outputs are then conditioned through an inverse DOF to provide the individual actuator valve commands. DOF software supports mixed control mode either in displacement or force control. A schematic view of the DOF control is shown in **Figure 5**. MAST is an over-constrained system since it has eight actuators operating to control six DOFs. In such system, the actuator displacements are constrained but there can be infinite number of force combinations for a given motion profile. Furthermore, the specimen often has very high stiffness, therefore small position offset could generate large distortion forces in different actuators. Therefore, another layer of force balance control is implemented to compensate the actuator servo valve commands and ensure the forces are distributed in a balanced manner among all driving actuators.

OpenFresco [7] can be coupled with various analysis software packages (e.g. OpenSees, Abaqus or Matlab) for computer representation of the complete structure. A “host” computer runs both the analysis software package and OpenFresco, and is connected to the physical specimen in the MAST payload through a “target computer.” OpenFresco connects directly with the MAST 6DOF control system through a ScramNet interface/shared memory card. Displacement feedback, force feedback and external signals from 1) the 6DOF system, 2) up to 4 ancillary actuators, and 3) up to 8 analog inputs, are shared directly with the “target” computer through the ScramNet interface. The analysis software communicates through OpenFresco to send and receive control signals to the “target” computer, provide new targets, and receive feedback from the MAST 6DOF Controller.

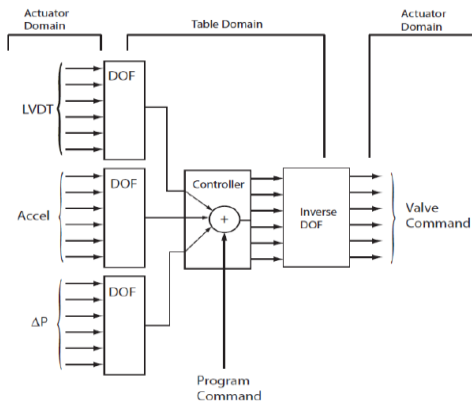


**Figure 5:** Schematic of MTS DOF control

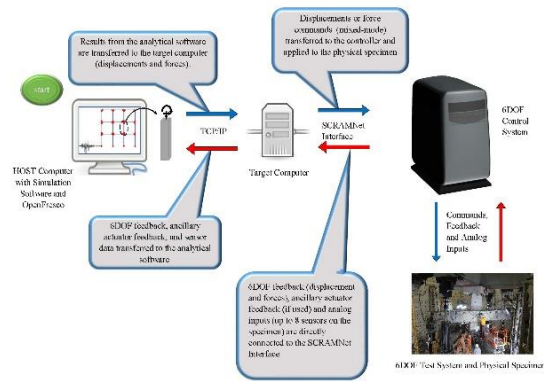


**Figure 6:** Schematic Hybrid Simulation Control

The predictor-corrector algorithm [7] provides the synchronization of the FEA numerical integration and the actuator control processes. Often, the integration step size ( $dt_{int}$ ) is larger and the control step size ( $dt_{con}$ ) is smaller. For slow hybrid simulation, a third time step needs to be defined as simulation step size ( $dt_{sim}$ ), which can be hundreds or even thousands times the integration step size ( $dt_{int}$ ) for multi-axial testing of very stiffness specimen. The predictor-corrector algorithm is an event-driven solution strategy implemented in Simulink and executed in realtime Target PC. At the beginning of each FEA integration step before the response is available, the predictor mode drives actuators utilizing extrapolation from past data. Once the FEA is completed, the corrector mode is activated to perform interpolation and drive the actuators to the desired displacement states. In the less likely situation when the integration takes longer than the simulation step size, the algorithm adapts and switch to slowdown mode without aborting the test abruptly.

## MAST HYBRID SIMULATION CASE STUDY AND VALIDATION

A three-story L-shape steel moment resisting frame structure is used in the hybrid system validation tests. The structural story height is 5.5 m (18 ft) and bay width is 9.5 m (31.2 ft) in both  $X$  and  $Y$  directions, with three bays in the  $X$  (east-west E-W) direction and two bays in the  $Y$  (north-south N-S) direction. The strong axis of the columns is in the N-S direction. The steel columns are W12×190 ASTM 572 Gr. 50 (345 Mpa) section, the column bases are modelled as fixed at the ground level. The building floor system is comprised of W12x106 steel beams acting compositely with the floor slab. In accordance with common practices, the rigid floor diaphragm assumption is implemented as multi-point constraints in OpenSees at each column beam joint node. The inertia effects are represented as concentrated mass of 25 tons at the column beam joints. The

resulting structural natural frequencies and mode shapes are shown in **Table 2** and **Figure 7**, respectively. The Raleigh damping ratio of 5% is assumed for the first two modes.

**Table 2: Structural Dynamic Modes**

Dynamic Mode no.	1	2	3	4
Natural Freq. (Hz)	0.59	0.75	1.88	2.70

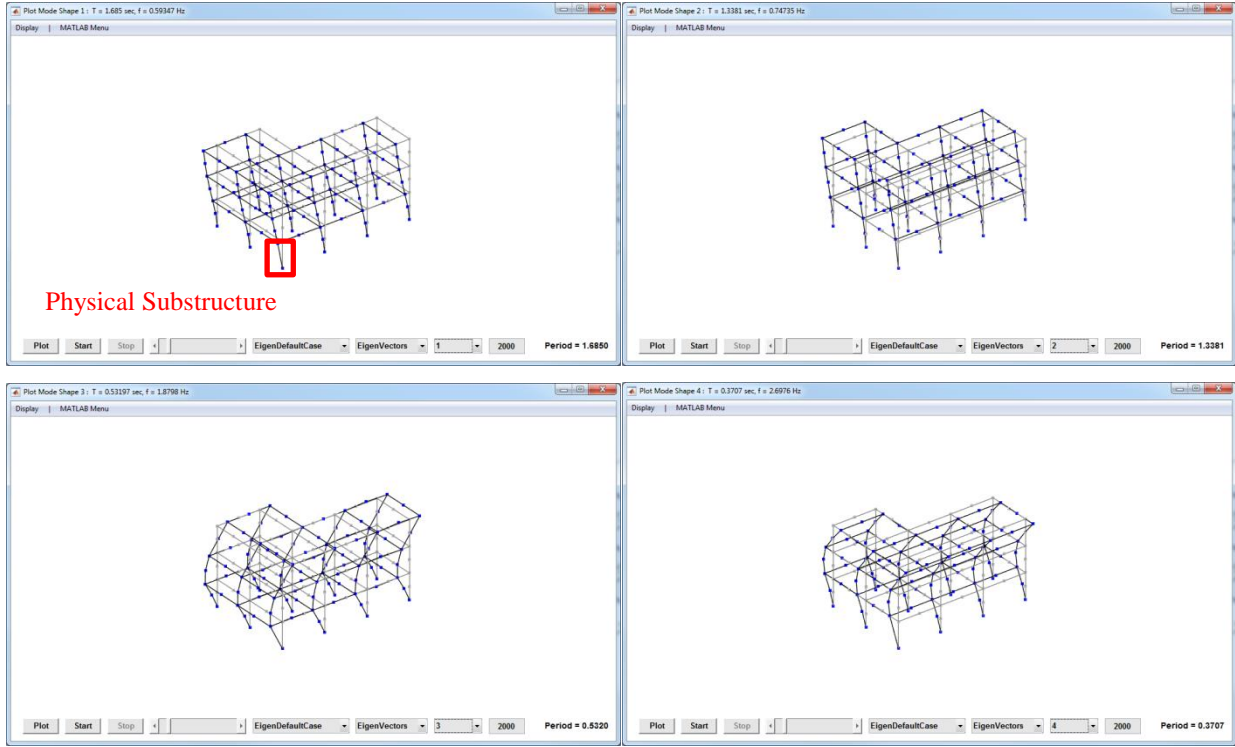


**Figure 7: Structural Dynamic Mode Shapes**

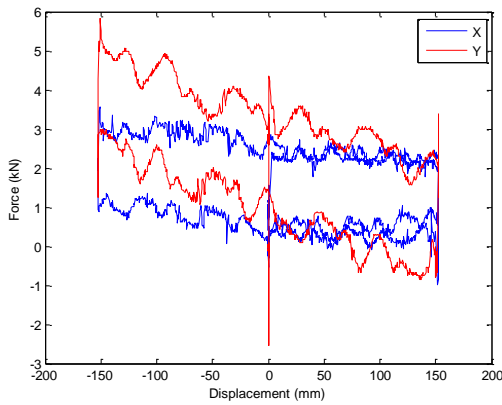


**Figure 8: Quasi-static cyclic testing – no specimen**

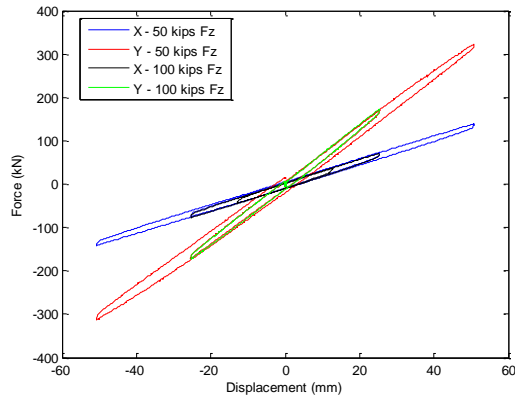


**Figure 9: Quasi-static cyclic testing – with specimen**

**MAST System Friction Characterization**

The quasi-static ramp and hold cyclic tests are conducted to characterize the MAST system friction. The crosshead is first moved without the specimen but the vertical actuators support the crosshead self-weight (418 kN). The cyclic lateral displacements are imposed in X and Y direction, with the maximum displacement 152.4 mm (6 in). The measured force bands in **Figure 8** show the friction in both X and Y directions are less than 4.5 kN (1 kip), which is considered very low for the system of such large size. The unique design of hydrostatic bearings in vertical actuators enables this ultra-low friction feature, making the system ideal to perform high performance hybrid simulation without the necessity of laborious friction

compensation efforts. Friction could be a major challenge for multi-axial loading system of such size, which could cause hybrid system instability if not properly managed.

Cyclic tests are conducted again after the specimen is installed. The maximum imposed lateral displacements are 50.8 mm (2 in) and 25.4 mm (1 in), with applied vertical force  $FZ$  of 222 kN (50 kips) and 445 kN (100 kips), respectively. The measured forces  $F_X$  and  $F_Y$  in **Figure 9** shows good repeatability under different motion and force combinations. The  $F_X$  and  $F_Y$  hysteresis bands are less than 15 kN (3 kips), which shows the system friction is still quite low even with the large axial forces on the vertical actuators bearings.

### MAST System Hybrid Simulation Results

In the hybrid simulation test cases, the vertical DOF  $Z$  is controlled by applying constant downward load of 222 kN (50 kips) to simulate the gravitational effect. All other 5 DOFs ( $X$ ,  $Y$ ,  $R_X$ ,  $R_Y$ ,  $R_Z$ ) are in displacement control with commands generated from the numerical substructure. The earthquake records used N-S (360) and E-W (090) components recorded at Sylmar County Hospital parking lot in Sylmar, California, during the Northridge, California earthquake of January 17, 1994. The first test uses 50% Northridge earthquake records in both  $X$  and  $Y$  directions. Only the first 15 seconds of the earthquake data (this segment contains all earthquake peaks) is tested in order to shorten the run time. The AlphaOS generalized integration scheme is selected and the numerical integration time step is 0.01 sec. The comparison of pure FEA (solid lines) and hybrid simulation numerical substructure responses (dashed lines) are presented in **Figure 10**. The nodal displacements/rotation angles of all DOFs are compared at the interface node (the top of the physical column). Excellent correlations are observed between two sets of results. This test validates the experimental setup is representative of the analysis assumptions, e.g. the initial stiffness of the physical column is very close to the fixed-fixed boundary condition assumed in the FEA. The displacement in the  $Z$  direction is very small due to low excitation and the high axial stiffness of the column specimen. Therefore, the  $Z$  DOF controlled in force instead of displacement. In the future, it is desirable to have an accurate force control capability integrated in hybrid simulation framework. The rotational angle  $R_Z$  is small due to the rigid floor diaphragm assumption.

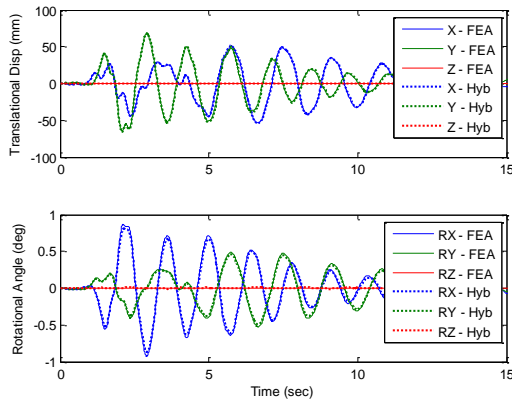


**Figure 10:** Pure FEA vs Hybrid Sim – 50% Northridge

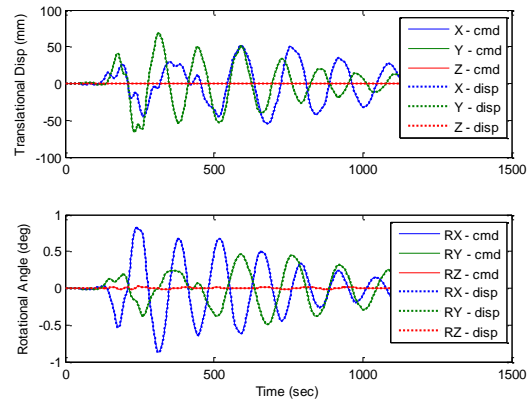


**Figure 11:** Measured command vs feedback – 50% Northridge

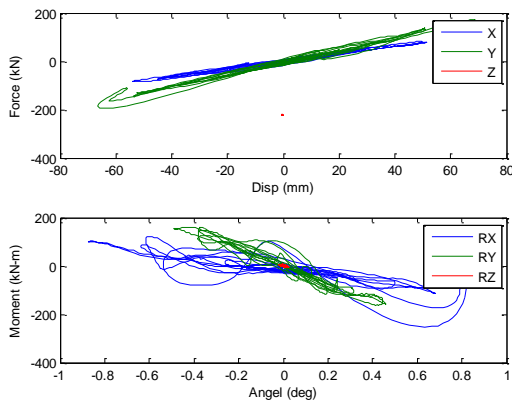


**Figure 12:** Force vs disp hysteresis – 50% Northridge

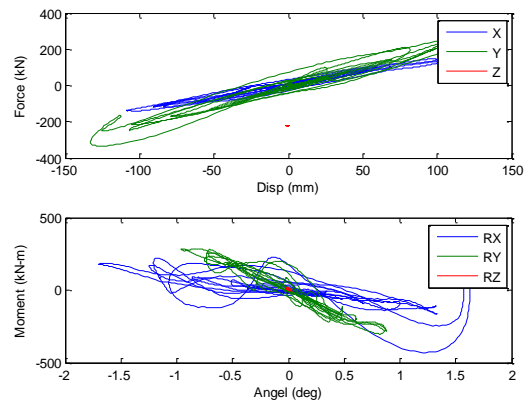


**Figure 13:** Force vs disp hysteresis – 100% Northridge

Under 50% Northridge, the measurements of commands and feedbacks of all DOFs are presented in **Figure 11**. The hybrid simulation is slowed down by a factor of 100, which is mostly determined by the maximum loading velocity of the MAST system. For each DOF, the feedback tracks the command very well without local instability or non-smoothness. It demonstrates the MAST is a high performance system, with small system imperfections including friction and cross-coupling etc. The measured force/moment and displacement/rotation hysteresis relations are presented in **Figure 12**. The  $X$  and  $Y$  responses are mostly linear under the 50% Northridge magnitude. The  $R_X$  and  $R_Y$  responses exhibit some hysteresis since they are more sensitive to the system imperfections.

Another hybrid simulation test run was conducted at 100% Northridge in  $X$  and  $Y$  directions. The hybrid simulation is slowed down by a factor of 200 in this run. The force and displacement hysteresis is presented in **Figure 13**, which shows noticeable nonlinear hysteresis in  $X$  and  $Y$  DOFs since the column starts to yield under the 100% earthquake magnitude. The strain measurements in **Figure 14** show the maximum is about 2500 micro-strain at 1/3 height of the column. It demonstrates the MAST system is quite capable of performing nonlinear tests on full-scale structural components.

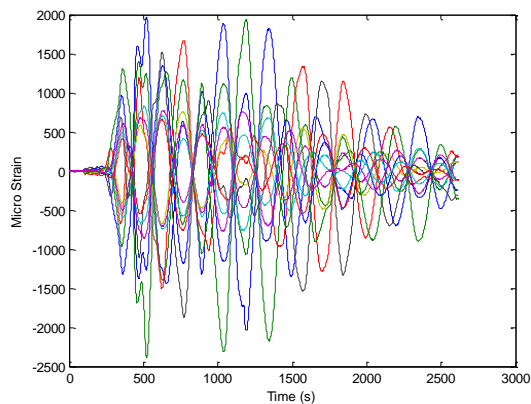


**Figure 14:** Strain measurements – 100% Northridge

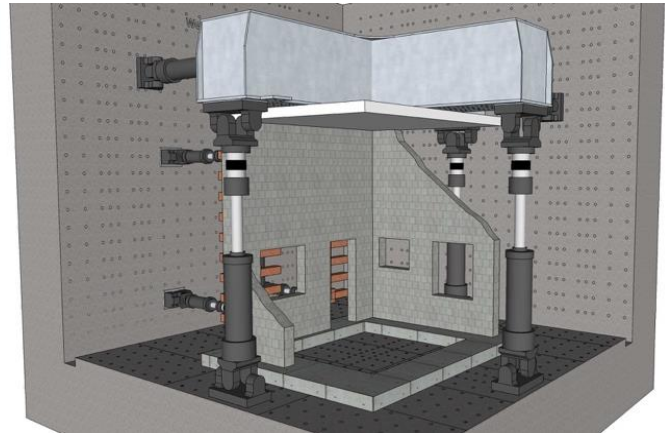


**Figure 15:** Envisioned masonry wall assemblage

## POTENTIAL FUTURE PROJECTS

Given the capabilities of the MAST system, a large number of testing needs can be satisfied. A few examples of specific systems that are envisioned for potential future testing are described here.

Masonry wall systems, with floor plans comprising multiple walls in orthogonal directions and with openings of various sizes have received little attention experimentally. Some of the obstacles to this type of test are the dimensions of such systems, and the difficulty to fabricate small- or medium-scale test specimens. Yet, unreinforced masonry structures and non-ductile reinforced masonry buildings are some of the largest hazards during strong ground shaking. The MAST Lab has the capability for handling masonry assemblages (**Figure 15**) of complex configurations at full-scale or near full-scale using hybrid simulation with “ramp-and-hold” loading. For simulation of wind loading, the ancillary actuators can be used to represent resultant wind forces arising from wind pressures on the walls. The front and sidewalls in **Figure 15** have been removed for clarity.

There is a dearth of physical data from controlled laboratory experiments on the response of large-scale timber structures subjected to simulated earthquake and wind loading. Tests such as that envisioned in **Figure 16** could be used to determine the mechanisms of resistance of the main structural load resisting systems (e.g., walls, frames) to loading from extreme events using the MAST apparatus. The system shown is a one- or two-story assemblage representative of timber construction that is commonly used in the United States for residential and light commercial construction. The system comprises stud walls made using nailed lumber and oriented strand board (OSB) sheathing, and timber floor diaphragms made using lumber joists (or fabricated timber floor trusses) and OSB sheathing. The system could be connected using nails, plates, metal hangers, tie-downs or other connectors intended to increase the resistance of the system to lateral loading. The specimen could include window and/or door openings in some of the walls (some of these elements and the OSB sheathing and stud framing have been removed for clarity in **Figure 16**). Whiffletree assemblages, driven by the ancillary actuators, could serve to simulate out-of-plane loading on the walls, and the loading procedure could utilize the MAST crosshead in a hybrid simulation framework to impose a history of lateral drift (or force) in one (or both) horizontal direction(s). In addition, the

other MAST DOFs would be defined so as to impose boundary forces or deformations at the top of the specimen that would be present in the prototype structure at that location.

A new line of research for the MAST Lab has been envisioned that would feature a large calibrated soil box that would enable testing of the response of soils in foundation systems (i.e. soil-structure interaction effects). The soil box can be constructed in the payload area of the MAST apparatus (**Figure 17**), with the sides of the box comprising stiff panels that are connected along their corners and with tensioned steel rods between the edges of the panels as needed to create stiff boundary conditions. Piles, footings or other foundations can be placed in the soil, and the top of these foundation elements can be connected to the MAST crosshead. The MAST crosshead could provide vertical loading at the top of the foundations, in a hybrid simulation scenario, along with appropriate boundary conditions. Additional loading can be applied to the bottom of the foundation elements using the ancillary actuators, or with dynamic shakers. Dynamic shakers can also be attached to the sides of the soil box to represent dynamic loading of the soils as in an earthquake. The front and side of the soil box in **Figure 17** have been removed for clarity.

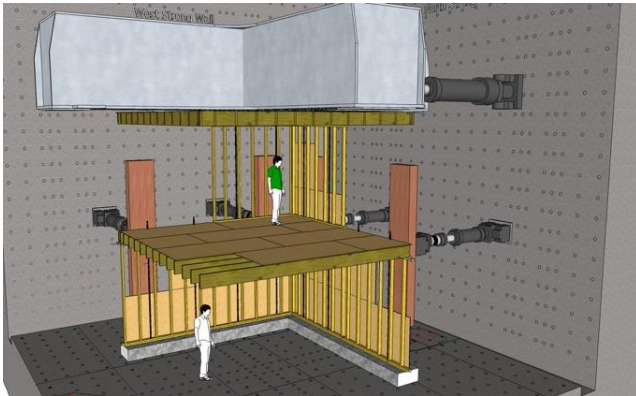


**Figure 16:** Idealized framed timber structure

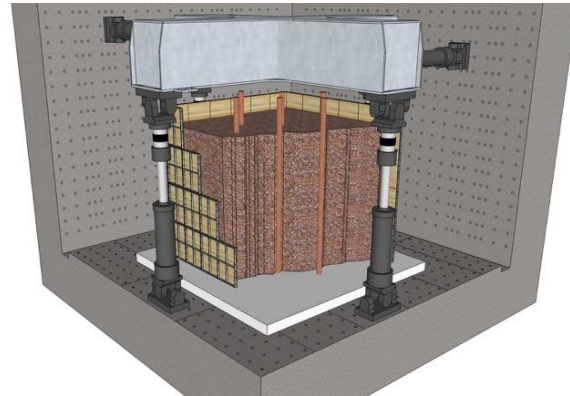


**Figure 17:** Idealized soil box in the MAST

## REFERENCES

- [1] Schultz, A.E. and Bergson, P.M. (2017). "State-of-the-Art Structural Testing for Simulated Earthquake and Wind Loading," *6th Structural Engineers World Congress, SEWC 2017*, Cancún, Mexico, November 14-17.
- [2] McKenna F., Fenves G.L., and Scott, M.H. (2000). *Open System for Earthquake Engineering Simulation*, Univ. of California, Berkeley, California.
- [3] Sritharan, S. (2017). "Hexcrete Tower for Harvesting Wind Energy at Taller Hub Heights - Budget Period 2." Report No: DOE-ISU-06737-1. Iowa State Univ., Ames, IA, May, 135 pp.
- [4] Simasathien, S. (2016). "Enhanced Seismic Performance of Special Truss Moment Frames and Staggered Truss Framing System for Seismically Active Areas." Ph.D. Dissertation, Univ. of Texas at Arlington, May, 433 pp.
- [5] Palmer, K.D. (2016). "Seismic Behavior, Performance and Design of Steel Concentrically Braced Frame Systems." Ph.D. Dissertation, Univ. of Washington, Seattle, May, 433 pp.
- [6] Thoen, B. 2013. *Generic Kinematic Transforms Package*. Minneapolis, MN: MTS Systems Corporation.
- [7] Advanced Implementation of Hybrid Simulation. Andreas Schellenberg, Stephan Mahin, Gregory Fenves, PEER report. 2009.